# Analysis of vehicle vibration sources for automatic differentiation between gas and diesel piston engines

Kevin J. Sigmund[a], Stuart J. Shelley[a], Mitchell Bauer[a], Frederick Heitkamp[b]
[a]Etegent Technologies, Ltd., 1775 Mentor Ave. Suite 302, Cincinnati, OH, USA 45212-3575
[b]AFRL/RYMMA, 3109 Hobson Way, Building 622, WPAFB OH, 45433-7700

## ABSTRACT

Vibration signatures sensed from distant vehicles using laser vibrometry systems provide valuable information that may be used to help identify key vehicle features such as engine type, engine speed, and number of cylinders. While developing algorithms to blindly extract the aforementioned features from a vehicle's vibration signature, it was shown that detection of engine speed and number of cylinders was more successful when utilizing a priori knowledge of the engine type (gas or diesel piston) and optimizing algorithms for each engine type. In practice, implementing different algorithms based on engine type first requires an algorithm to determine whether a vibration signature was produced by a gas piston or diesel piston engine. This paper provides a general overview of the observed differences between datasets from gas and diesel piston engines, and proceeds to detail the current method of differentiating between the two. To date, research has shown that basic signal processing techniques can be used to distinguish between gas and diesel vibration datasets with reasonable accuracy for piston engines of different configurations running at various speeds.

**Keywords:** Vibrometry, feature extraction, gas vs. diesel, fuel type

## 1. INTRODUCTION

Identifying vehicle features such as engine type, speed, and number of cylinders from vibrometry data is a challenging task. One approach is to develop algorithms based on a set of training data[1][2][3]. In reality, however, datasets will often not be available to train an algorithm. Additionally, the vibration signature from a single vehicle can vary significantly depending on the sensing location, state of engine degradation and tuning, engine operating conditions, structural loading, and many other parameters. Thus, the challenge innate to this work is robustly extracting meaningful features from vibrometry signatures that can vary significantly between "identical" vehicles without prior knowledge of the specific vehicle's characteristic vibration signature. The key to addressing this challenge is to utilize knowledge of the fundamental physics of reciprocating piston engines. This approach enables useful features to be extracted (such as engine speed, number of cylinders, and fuel type) that are consistent across different vehicle serial numbers, operating conditions, measurement locations, etc. This is done without training data and without a priori knowledge of vehicle design characteristics.

The work presented here focuses on classifying a vibration signature as being produced by either an internal combustion (IC) gasoline piston engine or an IC diesel piston engine. In addition to being another feature to aid vehicle identification, it was shown that for specific test cases, classification of fuel type can significantly improve performance of cylinder count and engine speed detection algorithms that are currently being developed in parallel with this work. This paper will first provide a basic technical overview of the algorithms currently being developed as a part of the effort to detect engine speed and number of cylinders. One method used to improve the performance of the engine speed detection algorithm for several gasoline sedans will then be summarized. Finally, several prominent diesel engine noise sources will be highlighted, followed by an outline of the current fuel type detection algorithm and its performance.

The current feature extraction algorithms are validated with test data recorded by accelerometers. Though these algorithms will likely require tuning for optimal performance with laser vibrometry data, it is hoped that the physical phenomena responsible for a vehicle's vibration signature will also be discernible in data collected by laser vibrometry systems.

## 2. CURRENT ALGORITHMS TO DETECT SPEED AND NUMBER OF CYLINDERS

In the present work, blind detection of an IC piston engine's speed and number of cylinders relies heavily on two assumptions: 1) half order frequency is the dominant harmonic pattern in the vibration spectrum, and 2) firing frequency is the dominant spectral peak in the vibration spectrum.

Here, half order frequency refers to the frequency at which a full engine cycle repeats, which is equal to half an engine's speed (RPM) in a 4-stroke engine. Half order frequency is present in almost all piston engine vibration signatures due to some degree of variation in the firing process from cylinder to cylinder[4]. In a 4-stroke piston engine, these variations create patterns that appear in the vibration spectrum as spectral peaks spaced at a frequency equal to half the engine RPM. If prominent enough, these spectral patterns are easily extracted via cepstral analysis. A cepstrum essentially highlights periodicity in the frequency spectrum. Thus, if each cylinder created the exact same vibration, spectral energy would be spaced at firing frequency rather than the frequency of a full cycle (half order), and the firing frequency pattern would be extractable via cepstral analysis. The following example helps visualize this concept. It should be noted that accelerometer data used for this example was recorded directly from an engine on a test stand; thus the data is quite clean and is for demonstration purposes only. In an actual vibrometry ATR application, vibration will be sensed on a vehicle's surface, not directly on the engine. Also, the following discussion will frequently use the terms "power stroke" and "firing event" which will be used differently than "cylinder combustion." The terms "power stroke" and "firing event" will be used in reference to the stroke of a piston during which it applies positive torque to the engine's crankshaft. As discussed later for diesel engines, many different vibration sources are present during the power stroke of a piston, and thus saying that the engine vibration response is due to "cylinder combustion" is not completely correct. Cylinder combustion may be a major vibration source, but it is not the only source of engine vibration during a cylinder's power stroke.

For the following example accelerometer data was recorded from the block of a 6-cylinder Cummins ISB-275 (herein ISB) diesel engine while it was running at 730 RPM. Using an engine output that signaled the start of each cycle, the engine block vibration during the power stroke of cylinder 1 was extracted from an arbitrary cycle of the accelerometer data and plotted in the top plot of Figure 1. This data was then repeated 12 times (two ISB engine cycles) to simulate a case where the engine block vibration response to all cylinder power strokes is identical, as shown in the bottom plot of Figure 1. Note that the extracted engine block response to the first cylinder's power stroke was approximate since residual vibrations were present from the previous cylinder's power stroke. However, the purpose of this demonstration is not to characterize the exact response of the engine block due to a firing event, but to show the effect of a realistic periodic engine event on the corresponding spectrum and cepstrum.

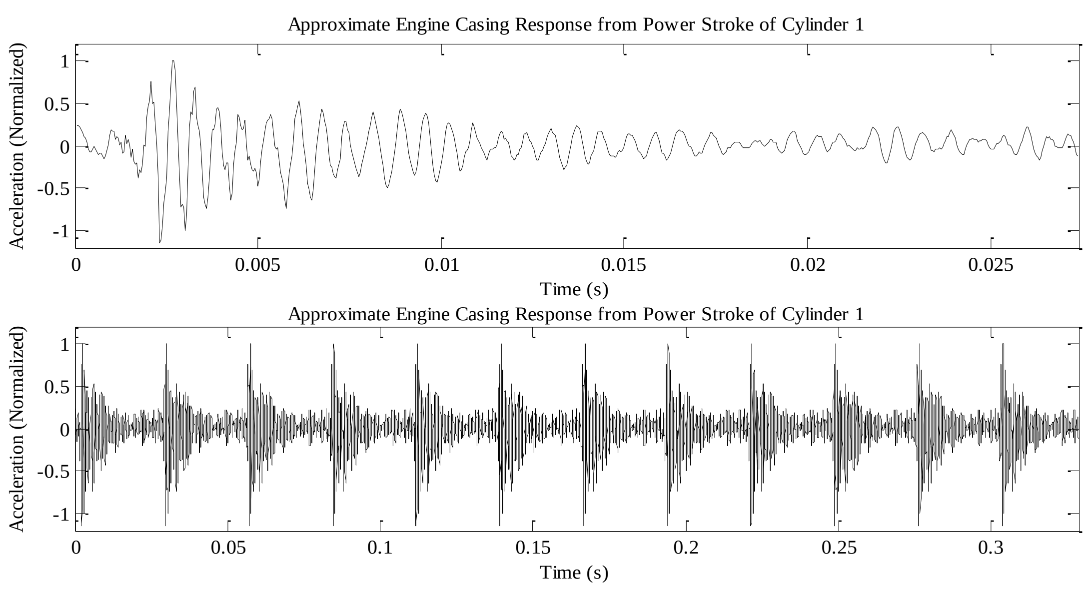


Figure 1: Measured engine block acceleration from cylinder 1 firing event (top),
single pulse repeated to simulate identical response from subsequent cylinder fires (bottom)

The time duration of the single extracted firing event response is 0.0274 s. Thus, repeating the response creates a periodic signal with a fundamental frequency of 36.5 Hz, which corresponds to the firing frequency of the 6-cylinder ISB running at 730 RPM. As depicted in Figure 2, this periodic signal contains spectral energy at harmonics of 36.5 Hz and, at corresponding frequencies, is equal in magnitude to the spectrum of the single firing event. The resulting pattern is then reflected in the cepstrum (Figure 3) as a strong 3rd order peak that corresponds to firing frequency. Note that harmonics of the 3rd order peak are visible as well. These are harmonics because in the quefrency-axis of the un-scaled cepstrum, peaks appear at 0.0274 s, 0.0548 s, etc. Thus, assuming half order frequency is dominant, RPM may be calculated as 4380 RPM and 2190 RPM, respectively ($RPM = 120/t$). As a result, harmonics in the time domain appear as subharmonics after converting to RPM. If all cylinder power strokes produced identical vibration responses in every vehicle, then the cepstral peak corresponding to the highest order could always be selected as firing frequency. However, this is not the case and often half order is the most dominant spectral pattern, which creates a dominant cepstral peak relating to half order frequency rather than firing frequency. Thus for example, if the 3rd order peak is selected, the engine speed extraction algorithm will think the vibration data was obtained from a vehicle running at 4380 RPM rather than 730 RPM. Remember that the algorithm assumes the 3rd order peak relates to half the engine rpm, and thus since the ISB has 6 cylinders, the predicted engine speed will be 6 times the actual engine speed (4380 / 730 = 6).

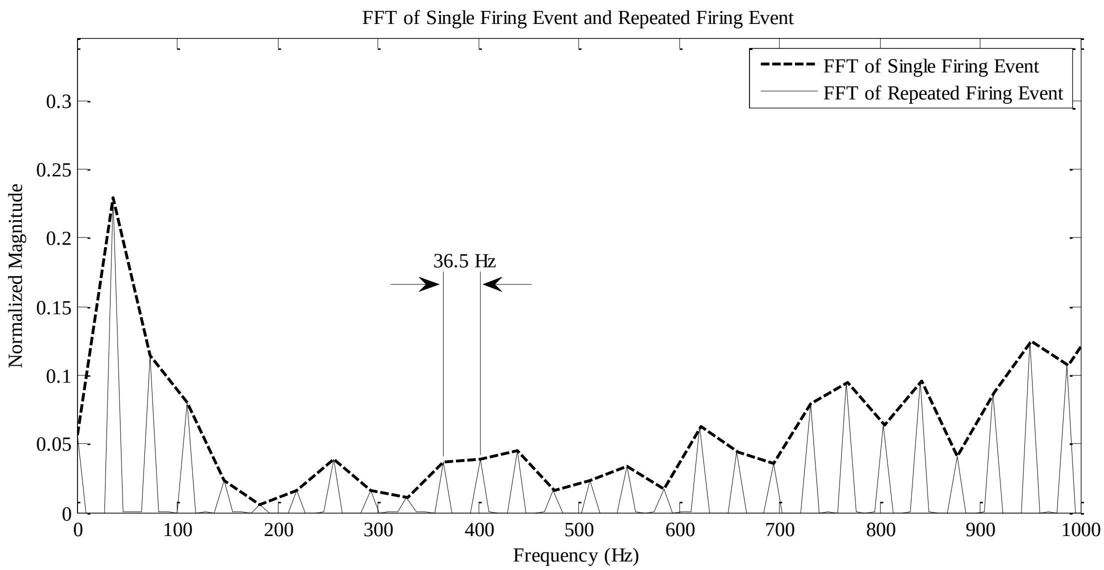


Figure 2: Spectrum of response from single firing event and repeated firing event

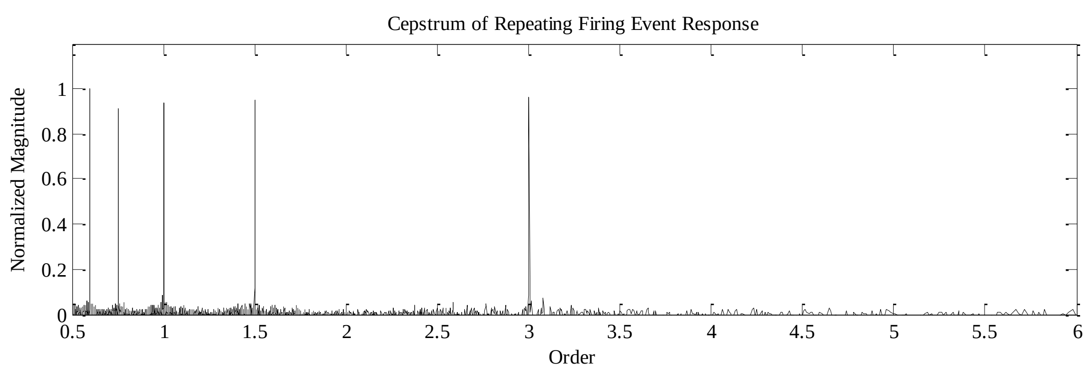


Figure 3: Cepstrum of repeated firing event

Next, to show the cepstral and spectral effect of cylinder to cylinder variations in the engine block response, similar analysis was performed on vibration data for two engine cycles that started with the same single firing event response used in the previous example. The extracted engine cycles are plotted in Figure 4. Though not immediately obvious by inspection, the engine block response does show cycle to cycle similarities and cylinder to cylinder variations. The most notable is the response from the power stroke of cylinder 6, which appears different than the responses from the power strokes of cylinders firing before and after, but similar to itself in the subsequent cycle.

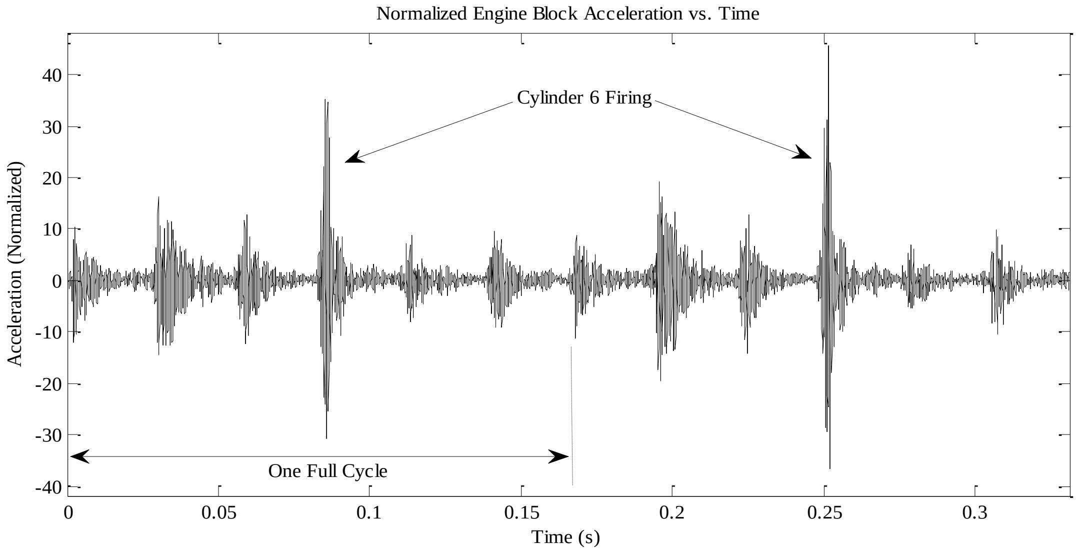


Figure 4: Accelerometer data from two cycles of ISB - 275 Cummins diesel engine running at 730 RPM

Figure 5 shows the corresponding spectrum and cepstrum of the two engine cycles from Figure 4. Note that the spectrum contains energy spaced at half order frequency and the dominant peak corresponds to firing frequency (3$^{rd}$ order). The half order spectral pattern is clearly visible in the cepstrum as a dominant peak corresponding to half order frequency. It is important to note that the order-axis of Figure **5** cannot show information lower than half order frequency because only two four-stroke engine cycles were included in the analysis; only two engine cycles were included in this example so that the response of each cylinder fire would be clearly visible in Figure **4**. Extraction of the spectrum's dominant peak (firing frequency) and the cepstrum's half order peak provides enough information to correctly compute engine speed and number of cylinders for many cases. Again it is important to recall that the goal of this work is to extract these features from vibration data sensed from the surface of a vehicle, and thus the vibration signature is often contaminated by other sources and not as clean as in the previous examples. Nevertheless, cylinder to cylinder variation is still often detectable on a vehicle's skin and in many cases additional processing techniques can be used help to eliminate content that is not of interest.

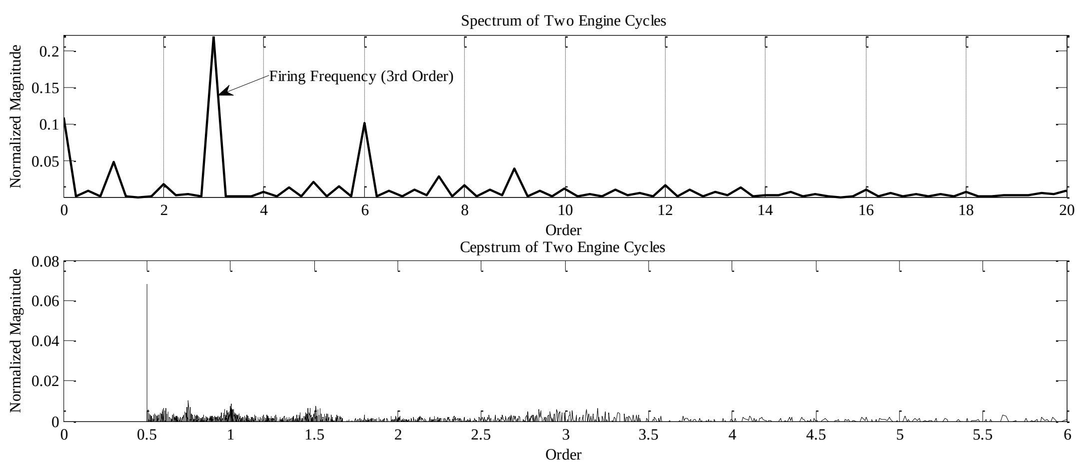


Figure 5: Time history, spectrum, and cepstrum of accelerometer data from inline 6-cylinder Cummins ISB-275 diesel engine running at 730 rpm

### 2.1 Motivation for Differentiating Between Gas and Diesel Vehicles

As previously mentioned, there are two factors motivating development of algorithms to automatically detect the fuel type from the vibration signature of piston engine vehicles. Firstly, the classification of gas or diesel fuel types is another feature that may be used to identify a specific vehicle. Secondly, it was found that extracting engine speed and number of cylinders was more successful when using different algorithms for gasoline vehicles than for diesel vehicles.

The dataset available for analysis contained, among other vehicles, vibration data from six different gasoline sedans. All of these sedans were powered by 4-cylinder engines with the exception of one, which was powered by a 6-cylinder engine. Data from most of these sedans shared an interesting characteristic, which was that a dominant cepstral peak corresponding to firing frequency was sometimes selected by the feature extraction algorithm instead of the correct half order peak. For example, Figure 6 shows the time history and corresponding cepstrum of accelerometer data taken from the skin of a 4-cylinder Toyota Corolla. The time history shows accelerometer data from approximately four engine cycles; this is approximate because no method was available to detect the start of an engine cycle. By inspection, the response of the Corolla's skin looks very similar for all cylinder firing events. This is reflected in the cepstrum, where the dominant peak corresponds to 3804 RPM which is four times the correct engine speed of 951 RPM. Note that the cepstrum does show either a harmonic of the firing frequency or some cycle to cycle similarity, which is indicated by the size of the peak corresponding to the correct RPM (951 RPM). The amplitudes of cepstral peaks that are harmonics or subharmonics of the correct engine speed are extremely sensitive to inclusion or omission of cylinder fires in the time history processed. In other words slight modification of the time history's length from that shown in Figure 6 can drastically change the amplitudes of cepstral peaks related to engine RPM. Thus, it is desirable to identify a robust method of detecting whether the firing frequency or half order frequency is the dominant spectral pattern.

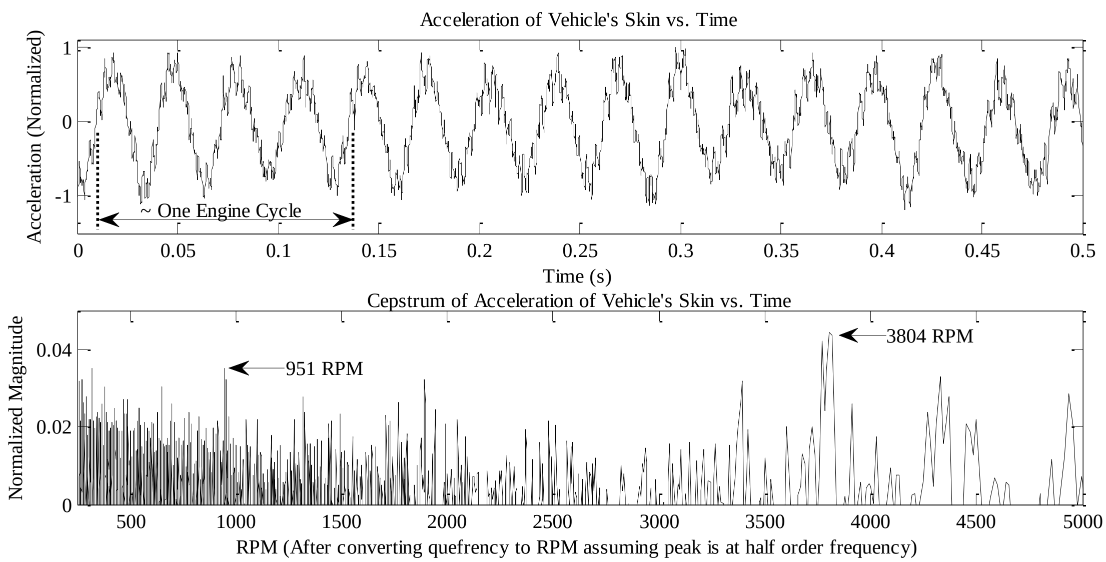


Figure 6: Time history and corresponding cepstrum of accelerometer data from the skin of 4-cylinder Toyota Corolla

While researching the aforementioned issue, it was observed that the autocorrelation of most vibration data from the sedans closely resembled a sinusoidal signal. Figure 7 shows the autocorrelation of the Corolla's time history from Figure 6. Inspection of this autocorrelation shows that the time lag between peaks is 0.0315 s, which corresponds to the Corolla's firing frequency while operating at 951 RPM.

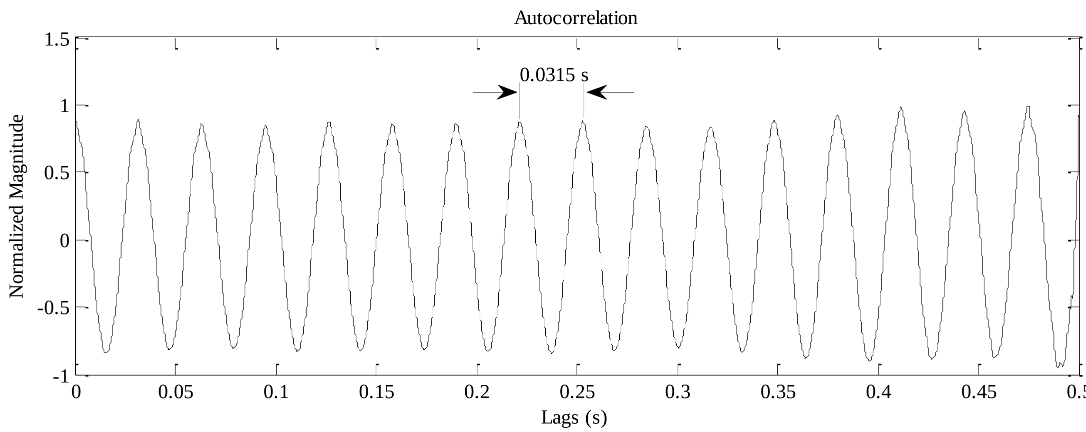


Figure 7: Autocorrelation of accelerometer data from a 4-cylinder Toyota Corolla

Though autocorrelations computed using data available from diesel vehicles sometimes showed visible peaks at firing frequency, they were never as sinusoidal as autocorrelations computed from the gasoline sedan data. Thus, the rationale was that if the algorithm knew the data was from a gasoline vehicle, dominant cepstral peaks could be used to extract a portion of the corresponding autocorrelation, and the number of cylinder fires could be estimated. For example, in the Corolla's case, the cepstral peak at 3804 RPM corresponds to a time value of 0.0315 s. Extracting a time block of 0.0315 s from the autocorrelation in Figure 7 yields, at most, a single cylinder fire. As a result, the algorithm could classify the vehicle as being a single cylinder vehicle running at 3804 RPM, or it could select another cepstral peak and reevaluate. When the cepstral peak at 951 RPM is selected, a 0.126 s time block is extracted from the autocorrelation, which encompasses four cylinder fires. After exploring other possible combinations, the algorithm decides that a 4-cylinder engine running at 951 RPM is most likely the correct classification. Implementation of this method increased correct engine speed detection of the five inline 4-cylinder sedans from an average of 55.2% correct engine speed detection to an average of 78% correct engine speed detection. Unfortunately, the 6-cylinder sedan was reduced from 70% correct engine speed detection to 59% correct engine speed detection. The method detailed above is difficult to implement on the available datasets from diesel vehicles since many of the autocorrelations do not contain distinct, dominant peaks at firing frequency. Thus, extracting subsets of the autocorrelation often results in the inclusion of additional peaks that are difficult to separate from the peaks corresponding to firing frequency.

It should be mentioned that, for the dataset being used at the time research began on fuel type differentiation, most of the gasoline vehicles were sedans, and the initial hypothesis was that the observations described would be common to many gas vehicles. However, it is possible that the decision to implement the described algorithm could just as easily be made based on a classification as a sedan rather than classification of fuel type. This hypothesis stems from the fact that data from additional gasoline vehicles has been inspected since the onset of this work. These vehicles are significantly different than the sedans and the aforementioned method of verifying the cepstral peak with the autocorrelation is not robust. However, after classification of gas or diesel, it may be possible to analyze the autocorrelation to make an additional classification as to whether or not the vehicle is a small sedan. Research to address this issue is suggested in the future work section of this paper. Data from these additional gas vehicles was used to help validate the fuel type algorithm described later.

# 3. DIESEL ENGINE VIBRATION SOURCES

Sound and vibration produced by compression ignition (CI) diesel piston engines is a topic that has been, and continues to be, a challenging area of research. Nowadays, stricter emission regulations have made it more difficult to achieve acceptable sound emission levels from diesel engines[4][5]. Though many different diesel engine noise sources have been identified, research for this work frequently found the following three being cited as major contributors [5]-[9]:

- Combustion
- Mechanical piston slap
- Mechanical gear rattle

The work presented in the remainder of this paper was completed after developing a physical understanding of the aforementioned noise sources, which will be briefly detailed in the following sections. Some other examples of mechanical noise sources that will not be described in this paper are

- Axial shaft motion and impacts in the presence of helical gears
- Impacts from the valve train
- Impacts from bearings
- Impacts from the fuel injector train

Before proceeding, an important assumption must be highlighted. Recall that the purpose of this work is to extract features from mechanical vibrations measured on the surface of a vehicle. Mechanical vibrations measured from a section of a vehicle can vary significantly from the sounds emitted from the entire vehicle that are perceived by an acoustic receiver. Many researchers study diesel engine noise for sound quality improvement and thus refer to combustion, piston slap, etc. as sources of noise/sound. Though sound data is not being measured for the purpose of this work, it was assumed that many of the diesel engine noise characteristics would be measurable from subsets of the structure as mechanical vibrations.

## 3.1 Diesel Engine Combustion

Before summarizing the combustion process of a CI diesel engine it is helpful to be familiar with the following definitions[10]:

- *Injection period* - a period that begins when fuel first starts to spray into the cylinder and ends as soon as flow from the injection nozzle stops.
- *Ignition delay / delay period* - time between the start of the injection period and the appearance of a flame in the cylinder.
- *Period of rapid combustion* - occurs just after the appearance of a flame in the cylinder and is characterized by fuel burning very rapidly and creating a sharp pressure rise.
- *Third phase of combustion* - the period between maximum cylinder pressure and the point where combustion is complete.

The combustion process in a CI diesel engine proceeds as follows[10]:

1. Air is compressed through a volume ratio often between 12 and 20.
2. Diesel fuel is injected just before the piston reaches its maximum height in the cylinder, initiating the start of the injection period. (Often fuel injection is sustained for some time after the injected fuel has started burning).
3. The injected fuel mixes with the air in the cylinder during the delay period.
4. Fuel begins to combust, marking the end of the delay period and the beginning of the rapid combustion period.
5. Maximum cylinder pressure is obtained, marking the start of the third phase of combustion, which continues until combustion is no longer a constituent of the cylinder’s pressure.

An example of a pressure curve resulting from the CI diesel combustion process is depicted in Figure 8. In this figure, the full pressure curve is divided into its two constituents: 1) the *motored pressure*, which is due purely to the piston compressing and decompressing the cylinder's contents (assuming no heat loss), and 2) the *combustion pressure*. Note that the delay period exposes the top of the motored pressure curve, which is then followed by a sharp spike in pressure due to the period of rapid combustion. The period of rapid combustion is facilitated by the fact that ignition in a CI engine depends on local conditions in the cylinder, and thus the air-fuel (A/F) mixture can ignite at multiple points simultaneously, causing very rapid pressure rise. This results in an impulsive, high frequency input to the engine block, which is a major contributor to a diesel engine's characteristic combustion noise. Generally speaking, longer delay periods cause more fuel to be present at the start of combustion, which increases the rate of pressure rise. On the contrary, the A/F mixture in a normally operating SI gasoline engine is ignited by a spark, after which combustion proceeds smoothly as the flame propagates through the combustion chamber. In general, the rate of pressure rise in diesel engines tends to be higher than in normally operating SI gasoline engines [10].

Engine designers, however, have developed many methods of reducing combustion noise in diesel engines. Though these methods will not be detailed here, the basic premise is that reduction of the delay period reduces the impulsive nature of the pressure curve by lowering the rate of pressure rise at the start of combustion. This in turn reduces the high frequency content of the combustion event and ultimately reduces the combustion knocking sound characteristic of CI diesel engines. Some methods of reducing the maximum rate of pressure rise include modifying A/F ratio, fuel system characteristics, compression ratios, etc[5]. The advent of turbochargers greatly reduced combustion noise by increasing cylinder pressure and reducing the delay period. As a result, combustion noise of turbocharged diesels is primarily a light load issue where boost pressures from turbochargers are low and the delay period is not significantly affected[5][7].

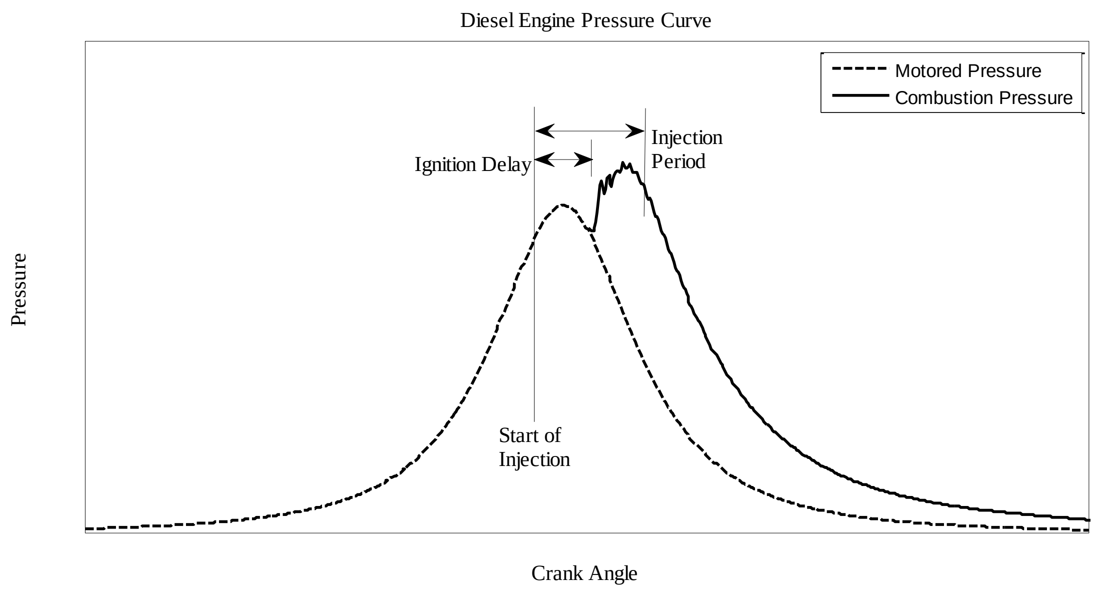


Figure 8: Diesel engine pressure curve (not necessarily representative of all diesel engine pressure curves)

### 3.2 Piston Slap

This section introduces the concept of piston slap as a source of noise and vibration in a diesel engine. Figure 9 shows the slider crank mechanism as the piston is about to complete its compression stroke and reach top dead center (TDC).
In this stage of the engine cycle, the cylinder pressure causes compression in the connecting rod (the compression pressure on the piston is larger than the inertial load of the decelerating piston), which in turn pushes the piston against the left cylinder wall (antithrust side); the antithrust side resists this force with the reaction force, $F_{cw}$. The instant the piston crosses past TDC, the horizontal component of the connecting rod's compression force switches directions and rapidly accelerates the piston towards the opposite cylinder wall (thrust side). As a result, the piston spans the clearance ($\delta$) and impacts the cylinder's thrust side, creating a high frequency impulsive input to the engine structure [6]-[9].

In [11], the response of a diesel engine casing to piston slap was predicted by applying a measured transfer function to the measured piston slap event. Experiments showed that, for the engine under test, piston slap was the primary source of engine casing vibration from approximately 600 Hz to 1500 Hz, and was a contributor between 100 Hz and 300 Hz. Marples[9] reported that researchers Griffiths and Skorecki found piston slap to be dominant in the 2– 4 kHz range while researchers Fielding and Skorechi showed that contributions from piston slap could be found up to 10 kHz.

Despite these findings, it seems logical that the frequency range of engine casing vibration dominated by piston slap will vary greatly depending on the engine design and operation. Some of the parameters that can affect the piston slap event's impulsive input to the engine block are engine block materials, piston materials, piston and engine block geometry, position of the piston pin (pin securing piston to connecting rod), operating clearances, peak cylinder pressures, etc.

Regardless, piston slap is a more prominent noise source in CI diesel engines than in SI gasoline engines. In fact, audible piston slap in an SI gasoline engine typically indicates the need for maintenance. The main reason for piston slap being a more prominent noise source in diesel engines is that higher peak cylinder pressures accelerate the piston laterally across larger operating clearances ($\delta$). As a result, the lateral velocity of a diesel engine's piston just before impact with the thrust side is greater than that of a gasoline engine[7]. It is worth noting that much of the literature found citing piston slap as a common noise source is quite dated. The authors of this paper have talked to experts who have hinted that piston slap may not be as prominent in modern diesel engines, though this has not been validated.

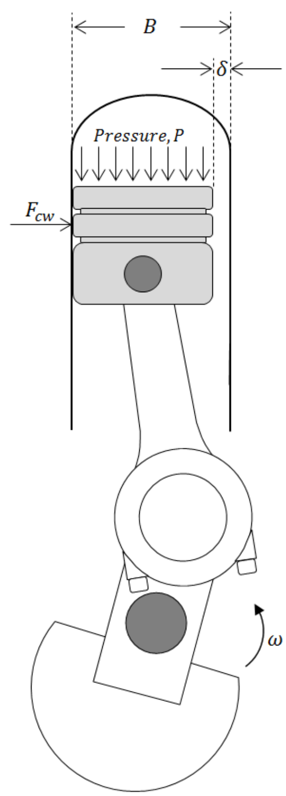


Figure 9: Slider crank mechanism showing cylinder pressure ($\boldsymbol{P}$), bore size ($\boldsymbol{B}$),cylinder wall reaction force ($\boldsymbol{F_{cw}}$), clearance between piston and cylinder wall ($\boldsymbol{\delta}$), and crankshaft rotational speed ($\boldsymbol{\omega}$)

### 3.3 Gear Rattle

Gear rattle is a phenomenon that occurs when torsional inputs cause the teeth of meshing gears to span operating clearances and impact their neighboring teeth. For durability reasons, many diesel engines use gears to drive the camshaft, fuel pump, etc[12]. In this application, gear rattle is often caused by torsional input from the crank and fuel system, and is thus tied to firing frequency[5]. To date, the authors of this paper have only identified gear rattle as an important diesel engine noise source and have not performed extensive research to determine the exact frequency range within which it is dominant or the most common causes of fluctuating torsional inputs.

# 4. AUTOMATIC DIFFERENTIATION BETWEEN GAS AND DIESEL ENGINES

## 4.1 Current Gas/Diesel Detection Algorithm

Unfortunately, mechanical and combustion sources of diesel engine noise are very difficult to separate, especially without detailed knowledge of the engine configuration and operating conditions. Furthermore, frequency content produced by mechanical and combustion forcing functions can vary significantly between engines of different builds, and even between different operating conditions of the same engine. Furthermore, the frequency content that reaches the surface of the engine is dependent on the transfer function between each cylinder and the outside of the engine casing. Even if the emitted noise/vibration was exactly the same for all engines, the transfer path from the engine to the skin of a vehicle is subject to drastic changes. Consequently, it is not practical to extract contributions of specific forcing functions from a vehicle's vibration signature to aid classification of fuel type.

For this work, however, separation of individual forcing functions of an engine is not necessary. Recall a few key observations about the diesel engine noise sources detailed earlier:

1. Combustion in a CI diesel engine typically results in a higher rate of pressure rise than in a normally operating SI gasoline engine[10], which results in audible sounds that are higher frequency.
2. Though it is likely not practical to pin down a precise frequency range within which piston slap is dominant, a piston slap event generally creates high frequency noise and is more common in CI diesel engines (according to older sources)[6]-[9].
3. Gear trains are more common in CI diesel engines and, torsional inputs cause gear teeth to impact impulsively, which in turn causes high frequency gear rattle occurring at firing frequency[5][12].

The key observations for this initial work are the fact that the above forcing functions produce high frequency content and that all of these forcing functions are tied to firing frequency. Thus, every power stroke of a diesel engine's cylinder will create a unique vibration signature with possible high frequency contributions from combustion, piston slap, gear rattle, etc. From the earlier discussion of periodic events, it follows that when the vibration signature of an individual cylinder's power stroke is repeated, its spectrum will be comprised of spectral energy equal in magnitude to that of the single pulse at the same frequencies and spaced at the frequency of the fundamental period. Recall that in the case of a 4 stroke piston engine, the power stroke of a single cylinder will occur every other engine revolution, thus the fundamental period corresponds to half order frequency.

These observations lead to the hypothesis that if a vibration signature was created by a diesel engine, then the high frequency portion of the corresponding spectrum should contain periodic half order energy. On the contrary, the high frequency portion of data from a gasoline vehicle would be expected to contain little half order content since the vbiration sources related to firing events typically exhibit lower frequency content. As a result, it seemed logical to analyze a low frequency and high frequency portion of a spectrum separately and check for strong periodic content that shared the same fundamental frequency. Again, the need to recognize spectral patterns justified the use of cepstral analysis. In short, the algorithm compares the cepstrum of the high frequency portion of the spectrum with the cepstrum of the low frequency portion of the spectrum and looks for dominant peaks in the same locations. The two cepstra of data from a diesel vehicle would be expected to have the same dominant peaks from both the high and low frequency portion of the spectrum while the two cepstra of data from a gasoline vehicle would not share the same dominant peaks.

The initial algorithm used a cutoff frequency of 800 Hz, which was determined empirically and is currently being optimized. A cutoff frequency of 800 Hz means that 0 – 800 Hz of the full spectrum was extracted to form the low frequency spectrum and >800 Hz of the full spectrum was extracted to form the high frequency spectrum. Next, a cepstrum was computed for each spectrum and the most prominent pattern was extracted. Figure 10 shows the cepstrum of both the high and low frequency spectra of a vibration signature from the skin of a 12-cylinder diesel vehicle. Note that the high and low frequency spectra look very similar and a strong peak corresponding to 2073 RPM and its harmonics (with respect to time, subharmonics with respect to RPM) are quite dominant. For this particular dataset, the developed fuel type detection algorithm would correctly classify the vibration source as being a diesel vehicle.

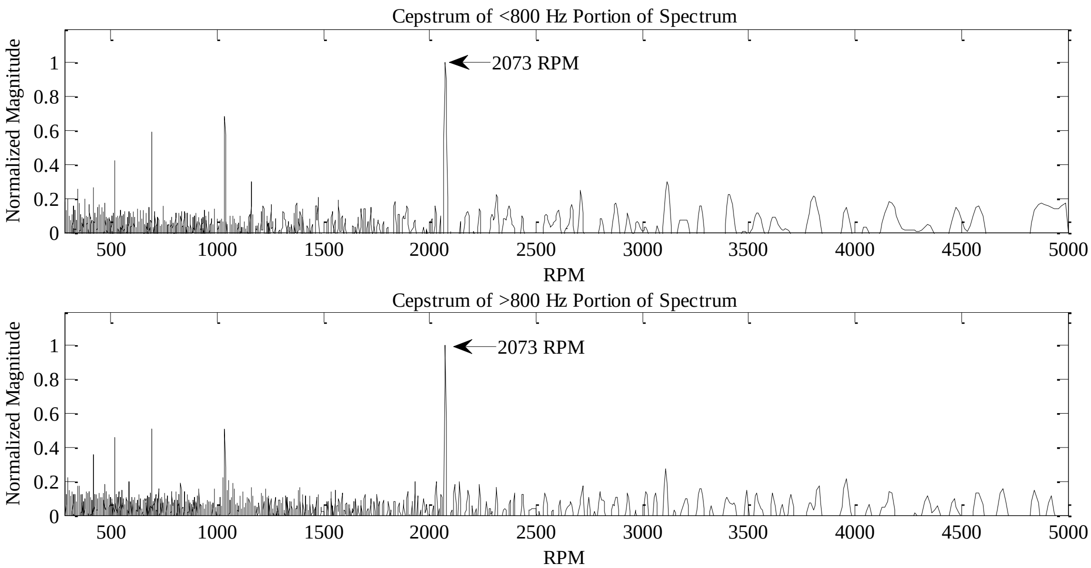


Figure 10: Cepstrum of both high and low frequency spectra of vibration signature from the skin of a 12-cylinder diesel vehicle

On the contrary, Figure 11 shows the cepstrum of both the high and low frequency spectra of a vibration signature from the skin of a 4-cylinder sedan. The algorithm currently being used to extract engine RPM was able to correctly identify the engine speed as 1153 RPM from the cepstrum of the low frequency spectrum, but was unable to find a similar pattern in the cepstrum of the high frequency spectrum. For this dataset, the fuel type detection algorithm would correctly classify the source as being a gasoline vehicle.

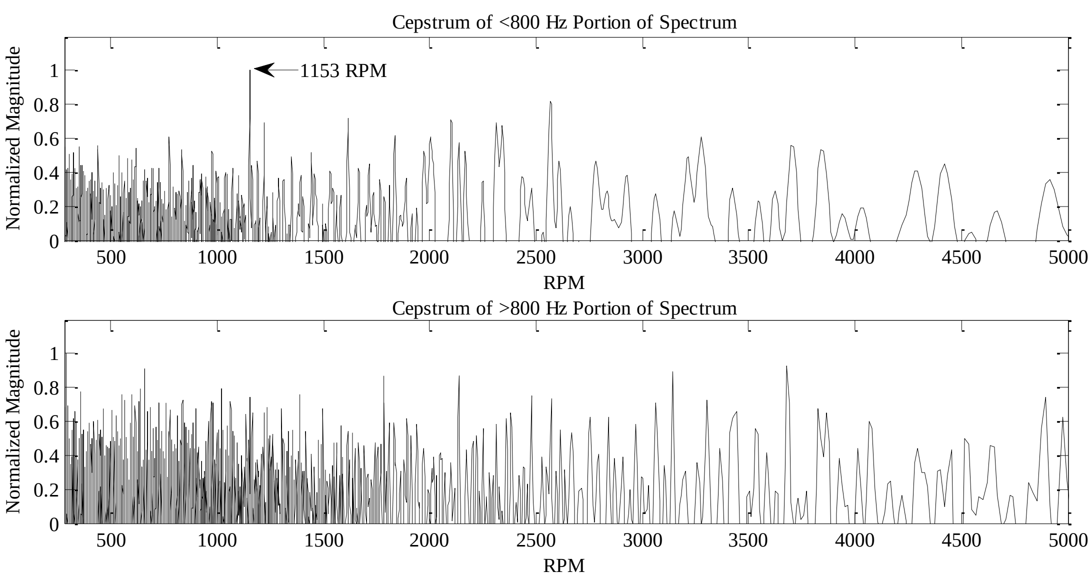


Figure 11: Cepstrum of both high and low frequency spectra of vibration signature from the skin of a 4-cylinder gasoline vehicle

### 4.2 Validation of the Current Gas/Diesel Algorithm

The aforementioned fuel type detection algorithm was tested on the accelerometer data available from 16 vehicles. Each vehicle was instrumented with between 5 and 20 accelerometers on its surface. No accelerometers located on the engine were used, with the exception of one dataset obtained from the ISB diesel engine on a test stand. Each sensor recorded between 10 and 60 seconds of data, which was divided into 1 second blocks. Each 1 second block was then processed by the fuel type detection algorithm. This resulted in approximately 160,000 samples of data for use in the validation process. It is important to note that the datasets on which the algorithm was tested came from vehicle operating conditions that varied from idle to full throttle. Again, it is assumed that the accelerometer data is relatively representative of actual laser vibrometry data and it is recognized that the use of laser vibrometry data could alter the performance of the fuel detection algorithm. This issue is briefly addressed in the future work section.

Results from the algorithm validation test are shown in Table 1, in which the Cummins ISB engine on a test stand is labeled as *Vehicle 1*. The algorithm performed well for many of the vehicles, but quite poorly for diesel vehicles 15 and 16. The algorithm's performance issue with these two vehicles has not yet been fully investigated. It is interesting to note, however, that operating conditions for these two vehicles make a significant difference in the algorithm performance. For example, benchmark results for vehicle 15 are categorized by operating condition in Table 2. Note that the fuel type detection algorithm performs very poorly at low operating speeds and significantly better at mid-range and full engine speed. Another interesting observation is that the algorithm performs better (though still poorly) on datasets from the hot idle operating condition than on datasets from the cold idle condition. This seems counterintuitive since one might think delay period and operating clearances would be greater in the cold idle condition, which would increase diesel engine vibration. Similar observations are made for vehicle 16, for which benchmark results are categorized by operating condition in Table 3. Interestingly, for the data available, significant dependence on operating condition is not common to all test vehicles. The algorithm performs well at most operating conditions for the other diesel vehicles tested and most large gas vehicles, with the exception of vehicle 12, on which the algorithm performs almost flawlessly at idle and very poorly at elevated RPM. Unfortunately, only data taken at idling conditions was available for the small 4-cylinder gasoline sedans, and thus conclusions cannot be drawn about the algorithm's performance for these vehicles at different operating conditions. Regardless, further research is required to fully understand failure modes and tune the gas/diesel detection algorithm for more reliable autonomous operation.

Table 1: Results from Benchmark Tests Run on Gas/Diesel Algorithm

| Vehicle | # of Cylinders | Fuel Type | % Correct Classification |
|---|---|---|---|
| **1** | 6 | Diesel | 100% |
| **2** | 6 | Gas | 99% |
| **3** | 4 | Gas | 99% |
| **4** | 8 | Gas | 99% |
| **5** | 12 | Diesel | 98% |
| **6** | 4 | Gas | 98% |
| **7** | 4 | Gas | 97% |
| **8** | 8 | Gas | 94% |
| **9** | 8 | Gas | 92% |
| **10** | 6 | Diesel | 89% |
| **11** | 4 | Gas | 81% |
| **12** | 8 | Gas | 77% |
| **13** | 6 | Diesel | 70% |
| **14** | 4 | Gas | 67% |
| **15** | 8 | Diesel | 34% |
| **16** | 8 | Diesel | 24% |

Table 2: Results from Gas/Diesel Benchmark Tests
on Vehicle 15 Categorized by Operating Condition

| **Vehicle 15 Operating Condition** | **% Correct Classification** |
|---|---|
| **Cold idle Test 1** | 1% |
| **Cold idle Test 2** | 2% |
| **Hot idle Test 1** | 16% |
| **Hot idle Test 2** | 10% |
| **Low rev (25% throttle) Test 1** | 29% |
| **Low rev (25% throttle) Test 2** | 28% |
| **Medium rev (50% throttle) Test 1** | 61% |
| **Medium rev (50% throttle) Test 2** | 66% |
| **High rev (75% throttle) Test 1** | 37% |
| **High rev (75% throttle) Test 2** | 35% |
| **Full rev (100% throttle) Test 1** | 64% |
| **Full rev (100% throttle) Test 2** | 66% |

Table 3: Results from Gas/Diesel Benchmark Tests
on Vehicle 16 Categorized by Operating Condition

| **Vehicle 16 Operating Condition** | **% Correct Classification** |
|---|---|
| **Cold Idle** | 1% |
| **Hot Idle** | 5% |
| **Idling in Gear** | 1% |
| **50% Throttle** | 61% |
| **90% Throttle** | 73% |

## 5. FUTURE WORK

There is significant research that could be conducted to improve the performance of the fuel type detection algorithm presented here. First and foremost would be to test the approach on a wider variety of vehicles. Recall that one of the initial motivations for this work stemmed from the fact that, for the initial dataset, correct identification of engine speed and number of cylinders was significantly improved for 5/6 gasoline sedans when using algorithms optimized for fuel type. However, another observation about these vehicles is that they are all passenger sedans, for which sound quality is an important issue. Thus, the potential exists that vibration data from the surface of a diesel powered passenger sedan exhibits characteristics similar in nature to vibration data from the gasoline powered passenger sedans studied for this work. In this case, classification of fuel type may be used for distinction between, say, a gasoline Volkswagen Jetta and a diesel Volkswagen Jetta, but may not be required for selection of a feature extraction algorithm optimized for fuel type. In other words, it may be more valuable to use the engine speed extraction algorithm discussed in section 2.1 based on whether or not the vehicle is a passenger sedan vs. whether or not the vehicle runs on gasoline. In addition to studying vibration data from diesel sedans, it would be helpful to have data from a wide variety of passenger vehicles (not just sedans), trucks, other heavy duty vehicles, etc. It is also suspected that further development of the fuel type detection algorithm would be greatly facilitated by multiple comparisons of very similar vehicles with different power plants, i.e. comparing a gasoline vehicle with a diesel vehicle of the same make and model.

Furthermore, the results for vehicles 15 and 16 in section 4.2 indicate that a study of the effects of various engine operating conditions is required. Additionally, results from the fuel type detection algorithm were not categorized by sensor location, and thus it is possible that correct classification of fuel type is sensitive to the location from which the data was obtained. Also, recall that the available dataset was processed in 1 second blocks. However, the effect of various time blocks should be investigated due to the observed sensitivity of peak amplitudes in the cepstrum to time history length.

Another important topic of research is the algorithm's performance when processing laser vibrometry data. Unlike the vibration data from accelerometers, which is collected from a small point on the vehicle, laser vibrometer systems measure vibration from an area encompassed by their beam. If data is obtained while measuring across vibration nodes, the velocity and phase will have odd symmetry. In this case, the result of spatially integrating the signal is an attenuated estimate of surface velocity [13]. Since higher frequency vibration can cause more closely spaced nodal points, there is a greater risk that the laser vibrometer's beam will encompass them. As a result, it is possible that some of the higher frequency content required by the current fuel type algorithm will be attenuated in the measured vibration signatures. As a result, it is important to study the accurate bandwidth of a laser vibrometry system at various ranges and determine how the fuel type algorithm is affected.

In general, there are many possible topics for future research in this area, and this section does not attempt to name them all or narrow the scope of the reader.

# 6. CONCLUSIONS

Overall, the work presented here provides groundwork for further development of an automated algorithm for use in classifying a vibration dataset as either being produced by a gasoline or diesel piston engine. Classification of a vehicle's fuel type may be leveraged to help identify a specific vehicle or determine an optimal algorithm to use for extraction of additional features such as engine speed and number of cylinders. One such case was presented in which correct classification of engine speed and number of cylinders was significantly improved when running an algorithm optimized for small gasoline powered sedans. Significant further research is required to optimize the performance of the presented fuel type detection algorithm. Topics for future investigation include sensitivity to vehicle type (especially small diesel passenger vehicles vs. small gas passenger vehicles), operating conditions, sensor location, data block size, beam size of laser vibrometer, etc. It is possible that future research will show that algorithms extracting engine speed and number of cylinders would benefit more from classification of vehicle configuration rather than fuel type. Regardless, classification of fuel type is an additional feature that may be used to identify a vehicle and it is hoped that this research can be used as a starting point for more robust fuel type extraction algorithms.

# REFERENCES


[1] Geurts, J., Ruck, D., Rogers, S., Oxley, M., Barr, D., "Autonomous Target Recognition Using Remotely Sensed Surface Vibration Measurements," SPIE 1955, 132-143 (2003).

[2] Stevens, M. R., Snorrason, M., Petrovich, D., "Laser Vibrometry for Target Classification," SPIE 4726, 70-81 (2002)

[3] Stevens, M. R., Stouch, D. W., Snorrason, M., Heitkamp, F., "Mining Vibrometry Signatures to Determine Target Separability" SPIE 5094, 10-17 (2003).

[4] Bodden, M., Heinrichs, R., "Diesel sound quality analysis and evaluation," ForumAcusticum, (2005).

[5] Reinhart, Thomas, "*Diesel Engine Noise Control Webinar,"* SAE International, Webinar I.D. #WB1041 Retrieved January, 2012, 1-91 (2011).

[6] Haddad, S. D. and Pullen, H. L., "Piston slap as a source of vibration in diesel engines," Journal of Sound and Vibration 34 (2), 249-260 (1974)

[7] Slack, W. James, "Piston slap noise in diesel engines," Massachusetts Institute of Technology, 11-20 (1982).

[8] Griffiths, W. J., Skorecki, J., "Some aspects of vibration of a single cylinder diesel engine," Sound Vib. 1 (4), 345-364 (1964).

[9] Marples, V., “On the frequency content of the surface vibration of a diesel engine,” Journal of Sound and Vibration 52 (3), 365-386 (1977).
[10] Taylor, C. F., [The Internal Combustion Engine in Theory and Practice: Volume 2: Combustion, Fuels, Materials, Design], Massachusetts Institute of Technology, Cambridge, 10-118 (1985).
[11] Lyon, Richard H., [Designing for Product Sound Quality], Marcel Dekker, Inc., NY, 127-132 (2000).
[12] Eberhard, P. and Ziegler, P., “Simulative and experimental investigation of impacts on gear wheels,” Comput. Methods Appl. Mech. Engrg., 197, 4653-4662 (2008).
[13] Jameson, D., Dierking, M., Duncan, B., “Effects of spatial modes on ladar vibration signature estimation,” Applied Optics 46 (30), 7365-7373 (2007).